OPTOELECTRONICS AND ADVANCED MATERIALS – RAPID COMMUNICATIONS Vol. 2, No. 8, August 2008, p. 459 - 465

Performance of a mid-infrared (MIR) SH-LED under high carrier injection

SANJEEV, P. CHAKRABARTI[a*]
Department of Electronics and Instrumentation Engineering, Institute of Engineering and Technology, MJP Rohilkhand University, Bareilly -243 006 India
[a]*Centre for Research in Microelectronics (CRME), Department of Electronics Engineering.,Institute of Technology, Banaras Hindu University, Varanasi -221 005 India*

In this paper, we present an analytical approach to evaluate the effect of high carrier injection on the performance of a mid-infrared (MIR) single heterojunction light emitting diode (SH-LED) based on P^+-$InAs_{0.36}Sb_{0.20}P_{0.44}$/ n^0-InAs/n^+-InAs material system for operation in 2.4–3.5 μm spectral range at room temperature. The model developed for the purpose takes into account all dominating radiative and non-radiative recombination processes, interfacial recombination and self-absorption in the active layer of the SH-LED structure. The effect of these processes on the quantum efficiency, modulation bandwidth and output power of the SH-LED under high carrier injection have been considered in this model. The output power of the SH-LED has been computed as a function of bias current and it is found to be in good agreement with reported experimental results.

(Received June 20, 2008; accepted June 30, 2008)

Keywords: Gas sensor, Optical fiber communication, Light emitting diode, Mid-infrared, Single heterostructure

1. Introduction

The mid-infrared (2-5μm) spectral region contains the strong fundamental absorption bands of a number of combustible and atmospheric pollutant gases like NH_3 (2.1 μm), HF (2.5μm), CH_4 (2.35 and 3.7 μm), N_2O (3.9 and 4.5 μm), SO_2 (4μm), CO_2 (4.27 μm) and CO (2.3 and 4.6 μm) [1]. These characteristics absorption properties are used in commercial gas detection systems based on optical absorption spectroscopy. Presently, the optical absorption based infrared gas detection techniques are becoming popular, as they are the only ones, which are truly gas specific and hence reliable for gas sensor instrumentation. Further, with the advent of polycrystalline metal halides such as Zirconium ($ZnCl_2$), Thallium Bromide and Thallium Bromoidide (KRS-5) and heavy metal fluoride glass (HMFG) based optical fiber, such as ZBLAN, which may offer a signal loss of less than 0.01dB/km in the mid-infrared region [2]-[4], renewed research interest is created to explore suitable mid-infrared sources which can be used in the futuristic optical fiber communication systems. The sources for mid-infrared spectral range require narrow bandgap semiconductor material for their fabrication. The major constraints in realizing the room temperature continuous operation source are the non-radiative recombination such as Shockley-Read-Hall (SRH) and Auger recombination process, which are the dominating recombination mechanisms for narrow bandgap semiconductor material system. Several double heterostructure junction [5]-[7], single heterostructure junction [8] and more recently, the homo-junction [9] mid-infrared light emitting diodes for various target wavelengths have been reported. However, systematic theoretical studies of these light emitting diodes have received little attention particularly, for their room temperature operation. It is, therefore, necessary to develop a generic model for the analysis of room temperature SH-LED operating in mid-infrared spectral region. As the technology of narrow bandgap semiconductors is not yet fully mature and the cost of experimental investigation is high, there is a need for further theoretical studies in the area in order to properly address the challenges ahead for the realization of room temperature SH-LED. The outcome of the theoretical studies will provide useful design guidelines for improving and optimizing the existing structures and developing new device prototype.

2. The proposed SH-LED structure

The device under consideration is the single heterostructure LED based on P^+-$InAs_{0.36}Sb_{0.20}P_{0.44}$/ n^0-InAs/ n^+-InAs material system. The schematic of the structure is shown in Fig. 1(a). It consists of a heavily doped (P^+) layer of quaternary materials InAsSbP of larger bandgap over the undoped InAs layer (active layer) of smaller bandgap to form the heterojunction. The whole structure is supposed to be grown on N^+-InAs substrate of the same conductivity as that of active region material. The energy band diagram of the heterojunction has been obtained by applying Anderson's model [10]. According to this model, the proposed structure forms a staggered

Type-IIb band alignment. The energy band diagram of the structure is shown in Fig. 1(b).

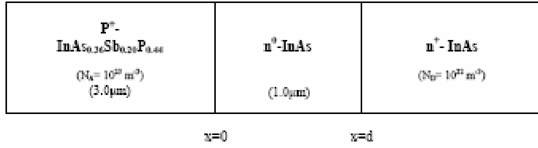

(a)

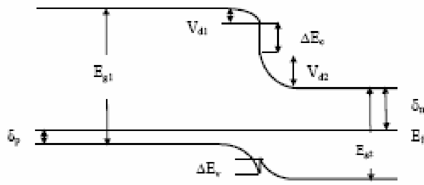

(b)

Fig. 1 (a) Schematic of the proposed SH-LED (b) Energy band diagram.

The energy bandgaps of the two semiconductors, their valance and conduction bandage discontinuity and built-in-potential at n^0-P^+ interointerface after formation of the heterojunction are related as

$$V_d = V_{d1} + V_{d2} \tag{1}$$

$$\Delta E_c = \chi_2 - \chi_1 \tag{2}$$

$$\Delta E_g = E_{g1} - E_{g2} \tag{3}$$

$$\Delta E_g = \Delta E_c + \Delta E_v \tag{4}$$

$$E_{g1} = \delta_p + \delta_n + V_d + \Delta E_c \tag{5}$$

where, V_{d1}, V_{d2}, V_d are the built in potentials on P^+ and n^0 sides and the total built-in-potential respectively, ΔE_g is the total band-edge discontinuity, χ_1 and χ_2 are the electron affinity values of the wide and narrow bandgap semiconductor respectively. E_{g1} and E_{g2} are the corresponding energy bandgap. δ_p and δ_n are the separation between the Fermi level and band edge on P^+ and n^0 side respectively. ΔE_c and ΔE_v are the conduction and valance band offsets of the materials, respectively.

3. Formulation of the model

The diffusion equation governing charge transport in SH-LED in the active region under forward bias is given by

$$\nabla^2\left(\Delta p(x)\right) = \frac{\Delta p(x)}{L_p^2} \tag{6}$$

where $\Delta p(x)$ is the injected hole density, L_p is hole diffusion length given by $L_p = \sqrt{D_p \tau}$, D_p is the hole diffusion coefficient and τ is the minority carrier lifetime. Equation (6) can be solved analytically using the following boundary conditions

$$\left.\frac{d\Delta p(x)}{dx}\right|_{x=0} = \frac{J}{qD_p} - \frac{s_p}{D_p}\Delta p(0) \tag{7}$$

$$\left.\frac{d\Delta p(x)}{dx}\right|_{x=d} = 0 \tag{8}$$

where J is the injected current density, q is the electronic charge, d is the thickness of active layer and s_p is the surface recombination velocity of holes at P^+-n^0 heterointerface. The hole density in the active region is calculated using equations (6), (7) and (8) as

$$\Delta p(x) = \frac{JL_p}{qD_p}\left[\frac{\cosh\left(\frac{d-x}{L_p}\right)}{\sinh\left(\frac{d}{L_p}\right) + \frac{L_p s_p}{D_p}\cosh\left(\frac{d}{L_p}\right)}\right] \tag{9}$$

The average hole density in the active region is given by

$$\overline{\Delta p} = \frac{1}{d}\int_0^d \Delta p(x)dx = \frac{J}{q}\frac{\tau_e}{d} \tag{10}$$

where τ_e is the effective carrier lifetime when surface recombination is important and is given by

$$\tau_e = \tau\left[\frac{\sinh\left(\frac{d}{L_p}\right)}{\sinh\left(\frac{d}{L_p}\right) + \frac{L_p s_p}{D_p}\cosh\left(\frac{d}{L_p}\right)}\right] \tag{11}$$

Equation (11) shows that there is a net reduction in the carrier lifetime due to the surface recombination. Here τ is the minority carrier lifetime given by

$$\frac{1}{\tau}=\frac{1}{\tau_R}+\frac{1}{\tau_A}+\frac{1}{\tau_{SRH}} \tag{12}$$

where τ_R, τ_A and τ_{SRH} are the values of radiative, Auger and SRH recombination lifetime of the minority carriers (hole) in the active region respectively.

3.1 Lifetime modeling

In order to calculate the dominant current components of SH-LED and to analyze the structure in terms of output power and modulation bandwidth, it is necessary to model various radiative and non-radiative recombination lifetimes of the carriers in the active region of the proposed SH-LED. We have taken into account all the three dominant recombination processes e.g., radiative, Auger and Shockley-Read-Hall (SRH) recombination mechanisms for computation of minority carrier lifetime. The SRH recombination can be largely controlled by improving the processing of the device while the Auger recombination lifetime is found to be dominating at room temperature for narrow bandgap materials. The modeling of the radiative recombination is rather straightforward. For direct band semiconductor, the radiative lifetime of the carrier can be expressed as

$$\tau_R=\frac{1}{B_r(n_0+p_0)} \tag{13}$$

where B_r is the radiative recombination coefficient of the material in active region, n_0 and p_0 are the electron and hole concentration in the active region under thermal equilibrium.

The modeling of Auger recombination lifetime is complex in nature. In the present model, we have assumed that the Auger processes involved in this case follow those observed in InSb-like band structure. For the sake of simplicity we have considered the three dominant Auger mechanisms e.g., Auger-1 (A-1) or CHCC process, Auger-7(A-7) or CHLH process and Auger-S (A-S) or CHSH process in the active region. The first two transitions occur at the lowest threshold energy $\left(E_{th}\cong E_{g2}\right)$ and the last transition is dominating in the material in which the spin split energy gap (Δ) is nearly equal to forbidden gap. In the structure under consideration, $\Delta=0.41eV$,which is close to the value of forbidden gap. Therefore, we have considered the effect of Auger-S recombination in the model. The lifetime of the carrier corresponding A-1, A-7 and A-S are given by

$$\tau_{A-1}=\frac{2\tau^i_{A-1}}{1+n_0/p_0} \tag{14}$$

$$\tau_{A-7}=\frac{2\tau^i_{A-7}}{1+p_0/n_0} \tag{15}$$

$$\tau_{A-S}=\frac{2\tau^i_{A-S}}{1+p_0/n_0} \tag{16}$$

where $\tau^i_{A-1},\tau^i_{A-7},\tau^i_{A-S}$ are the values of lifetime involving the above three Auger processes for the intrinsic materials, given by [11]

$$\tau^i_{A-1}=\frac{3.8x10^{-18}\varepsilon_s^2(1+\mu)^{1/2}(1+2\mu)exp\left[\left(\frac{1+2\mu}{1+\mu}\right)\frac{qE_{g2}}{kT}\right]}{\frac{m_e^*}{m_0}\left|F_1F_2\right|^2\left(\frac{kT}{qE_{g2}}\right)^{3/2}} \tag{17}$$

$$\tau^i_{A-7}=\frac{m_e^*(E_{th})\left(1-\frac{5qE_{th}}{4kT}\right)}{m^*_{eo}(1-\frac{3qE_{th}}{2kT})}\tau^i_{A-1} \tag{18}$$

$$\tau^i_{A-S}=\frac{5}{54}\frac{\varepsilon_s^2 m_{hh}^{*\,3} m_e^{*3/2}kT\Delta^2(E_{g2}+\Delta)}{\pi^4\hbar^3q^4n_i^2m_s^{5/2}(\Delta-E_{g2})exp\left[\frac{q(\Delta-E_{g2})}{kT}\right]} \tag{19}$$

Here, μ is the ratio of the conduction band to the heavy-hole valance band effective mass, ε_s is the permittivity, F_1 and F_2 are the overlap integrals of the periodic part of Bloch's functions, m_e^* is the electronic effective mass, m_0 is the electron rest mass, and n_i is the intrinsic carrier concentration, E_{g2} and Δ are the energy bandgap and spin-split-off energy of the material of the active region, $m_e^*(E_{th})$ is the electron effective mass corresponding to threshold energy for the Auger-7 transition. For this transition $E_{th}\approx E_{g2}$. For Auger-S transition m^*_{hh} and m_s correspond to the heavy-hole band effective mass and the spin-off band effective mass respectively.

The overall Auger lifetime value involving the three Auger processes can be obtained as

$$\frac{1}{\tau_A}=\frac{1}{\tau_{A-1}}+\frac{1}{\tau_{A-7}}+\frac{1}{\tau_{A-S}} \tag{20}$$

The lifetimes of minority carriers due to Shockley-Read-Hall (SRH) recombination can be modeled in terms of SRH trap-density and capture cross-section as

$$\tau_{SRH} = \frac{1}{\sigma N_f v_{th}} \tag{21}$$

where N_f is the SRH trap density, σ is the capture cross-section. Here v_{th} is the thermal carrier velocity of the minority carriers in the active region given by

$$v_{th} = \sqrt{\frac{3kT}{m_e^*}} \tag{22}$$

where m_e^* is the electron effective mass.

3.2 The current-voltage characteristics of the structure

The current through the forward bias SH-LED consists of two components:
(i) Diffusion current arising from the carriers injected from neutral P^+ to n^0 region and (ii) Drift current due to generation recombination in the depletion region at P^+-n^0 junction.

3.2.1 The diffusion component

Due to the presence of discontinuities at the bandages of the heterointerface, the diffusion current in heterostructure is different from that in homojunction. In the given structure, holes from P^+ region, having energy equal to the barrier $V_d - \Delta E_v$ can reach to the interface at n^0 region to constitute the total diffusion component of the current in the structure. The diffusion component of current is calculated by solving the standard one-dimensional diffusion equation (6) under forward bias using appropriate boundary conditions. The diffusion components of current due to injection of holes in n^0 regions can be obtained as

$$I_{sp} = q\frac{AL_p}{\tau_e} p_0 \frac{\left[\frac{L_p s_p}{D_p}\cosh\left(\frac{t-x_n}{L_p}\right) + \sinh\left(\frac{t-x_n}{L_p}\right)\right]}{\left[\frac{L_p s_p}{D_p}\sinh\left(\frac{t-x_n}{L_p}\right) + \cosh\left(\frac{t-x_n}{L_p}\right)\right]} \exp\left[-\frac{q(V_d - \Delta E_v)}{kT}\right] \tag{23}$$

where L_p is the diffusion length of holes, s_p is the surface recombination velocity for the holes at the interface, A is the device area, t is the thickness of the of InAsSbP layer and x_n and x_p are the widths of the depletion region on the P^+ and n^0 sides respectively.

The total diffusion current component for the structure is given by

$$I_d = I_{sp}\, exp\left[\frac{qV}{nkT} - 1\right] \tag{24}$$

where n is the ideality factor of the LED structure.

3.2.2 The generation-recombination component

The carriers generated in the depletion region are generally separated under the application of existing electric field. The transport of carriers across the heterojunction is strongly affected by the trap levels at the heterointerface inside the depletion region. The carrier generation-recombination in the active region is governed by the Shockley-Read-Hall equation. The current arising from the generation-recombination in the depletion region under forward bias is given by [12]

$$I_{gr} = \frac{2n_i WAkT}{(V_d - V)\tau_{SRH}} sinh\left(\frac{qV}{2kT}\right) \tag{25}$$

where V_d is the total built-in-potential, V is the applied voltage, $W\ (= x_n + x_p)$ is the total depletion width, which is the function of applied voltage V, n_i is the intrinsic carrier concentration of the active region.

4. Performance of the proposed SH-LED at high carrier injection

In this section, the effect of injected carrier density on the performance of the SH-LED has been modeled. Both radiative and non-radiative minority carrier lifetimes are affected significantly in the case of high level injection of minority carriers in the active region.

In presence of excess carrier (Δp), radiative lifetime can be expressed as

$$\tau_R' = \frac{1}{B_r(n_0 + p_0 + \Delta p)} \tag{26}$$

where B_r is the Radiative recombination coefficient, n_0 and p_0 are the electron and hole concentration in the active region under thermal equilibrium. Here Δp is given by

$$\Delta p = \left(\frac{J\tau_R'}{qd}\right) \tag{27}$$

here J is the injected current density. Solving (26) and (27) for the value of radiative recombination lifetime, we obtain

$$\tau_R' = \frac{\left[(n_0 + p_0)^2 + \frac{4J}{B_r qd}\right]^{1/2} - (n_0 + p_o)}{2J/qd} \tag{28}$$

Under the high injection condition, the lifetime values of three Auger processes can be obtained as [11]

$$\tau'_{A-1} = \frac{2n_i^2\tau^i_{A-1}}{(n_0+p_0+\Delta p)[(n_0+\Delta p)+\gamma(p_0+\Delta p)]} \tag{29}$$

$$\tau'_{A-7} = \frac{2n_i^2\tau^i_{A-7}}{(n_0+p_0+\Delta p)(p_0+\Delta p)} \tag{30}$$

$$\tau'_{A-s} = \frac{2\tau^i_{A-S}}{1+((p_0+\Delta p)/(n_0+\Delta p))^2} \tag{31}$$

where factor γ accounts for the hole-hole collisions and is given by

$$\gamma = \frac{\mu^{1/2}(1+2\mu)}{2+\mu} exp\left[-\left(\frac{1-\mu}{1+\mu}\right)\frac{qE_{g2}}{kT}\right] \tag{32}$$

Equations (29)-(32) show that there is a reduction in the value of the Auger recombination lifetime of minority carrier as we increases the carrier injection in the active region. This ultimately reduces the quantum efficiency of the device and limits the power output of the SH-LED at high carrier injection.

5. The power output and modulation bandwidth of SH-LED

The output Power P taking into consideration the variation of carrier lifetime due to heavy carrier injection, effect of surface recombination velocity, self-absorption into the active layer, of the SH-LED is given by

$$P = \eta h\nu\left(\frac{I}{q}\right) \tag{33}$$

where η is the quantum efficiency of the LED and I is the bias current.

The 3-dB modulation bandwidth (f_{3dB}) of SH-LED can be calculated as

$$f_{3dB} = \frac{1}{2\pi\tau_e} \tag{34}$$

6. Results and discussion

Numerical computations have been carried out for P^+-$InAs_{0.36}Sb_{0.20}P_{0.44}$/ n^0-InAs/ n^+-InAs single heterostructure light emitting diode (SH-LED) at room temperature. The values of different parameters used in the model are listed in Table 1. Some of the parameters of the quaternary materials (InAsSbP) have been computed from the parameters of the constituent binary/ternary materials using the linear interpolation formula.

Table 1. Values of parameters used in the model [9], [13]

Parameter	Value
N_A	$10^{24}m^{-3}$
N_D	$10^{22}m^{-3}$
T	3 μm
D	1 μm
σ	$10^{-19}m^2$
N_f	$10^{20}m^{-3}$
ε_r	15.15
ε_∞	12.3
E_{g1}	0.570 eV
E_{g2}	0.354 eV
χ_1	4.699 eV (estimated)
χ_2	4.9 eV
m_e^*	$0.023m_0$
m_p^*	$0.041m_0$
m_s	$0.16m_0$
m_{hh}	$0.41m_0$
Δ	0.41 eV

Fig. 2 depicts the forward-bias current-voltage characteristics of the proposed structure. The graph shows the usual exponential rise in the current with the increase in the applied voltage. The cut-in voltage is approximately 0.26 V.

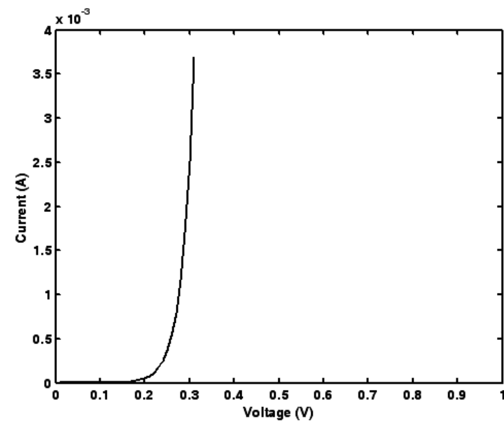

Fig. 2 Forward-bias current-voltage characteristics of the SH-LED

Fig. 3 shows the variation of the Auger and radiative lifetime of the carriers with the excess injected carriers. It is seen that the lifetime of carriers decreases drastically

with the increase in the excess injected carrier beyond $10^{24}/m^3$. It is also observed that Auger recombination lifetime decreases much faster than other non-radiative recombination lifetime and becomes dominating as we increases the injected carrier beyond $10^{25}/m^3$. Hence, it is dominating non-radiative recombination under high injection condition which affects the output power of SH-LED more severely.

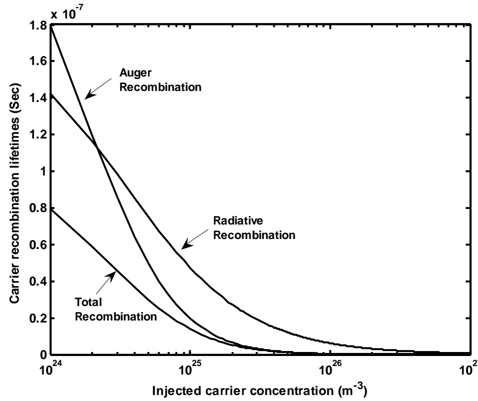

Fig. 3 Radiative and Auger recombination lifetime variation with the injected carrier concentration.

Fig. 4 shows the effect of various recombination mechanisms on the quantum efficiency of the SH-LED. The study reveals that the quantum efficiency of the SH-LED is greatly affected by the non-radiative recombination mechanisms such as SRH and Auger recombination. It is also seen that at room temperature operation the reduction in the overall efficiency is dominated by Auger recombination process. This in turn reduces the power output of the SH-LED.

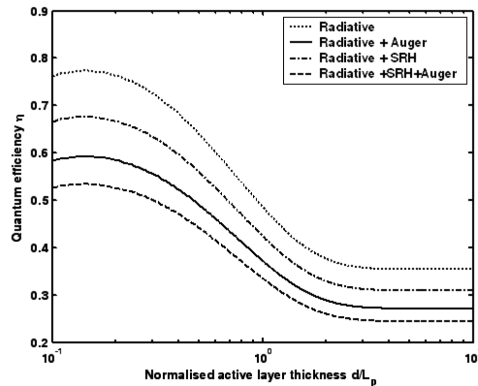

Fig. 4 The effect of various recombination mechanisms on the quantum efficiency of the SH-LED

Fig. 5 shows the variation of output power and bandwidth of SH-LED with normalized active layer thickness for two different recombination velocities (s_p=50m/s and 100m/s). It is seen that the bandwidth increases with the increase in active layer thickness for given values of surface recombination velocity. Further, with the increase in the surface recombination velocity for a given value of active layer thickness, the bandwidth increases. This increment in the bandwidth is on the cost of output power, so as to keep the output power-bandwidth product constant. In view of this, one has to optimize the device structure to meet the requirements in terms of output power and modulation bandwidth.

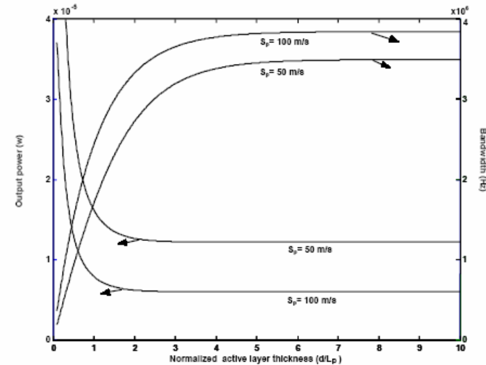

Fig. 5 Output power and modulation bandwidth variation with normalized active layer thickness for different surface recombination velocities.

Fig. 6 shows the variation of optical power output with the bias current. The experimental results reported by Krier et al. [9] for the same structure is shown by circles.

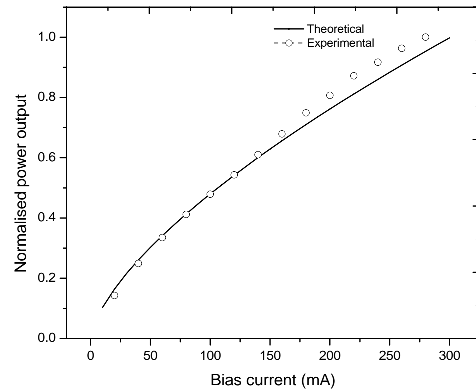

Fig. 6.Variation of optical power output of the SH-LED with the bias current.

It is found that theoretical results are in good agreement with the reported experimental results [9] particularly at low bias current level. For high bias current, high level of minority carrier injection takes place, which affect the minority carrier lifetime which in turn, reduces

the quantum efficiency and as a result output power of the SH-LED tends to saturate.

7. Conclusions

The study reveals that high level of carrier injection results in a reduction in the effective lifetime of the carriers which in turn causes the output power to saturate at higher bias current. It is found that the quantum efficiency of the SH-LED source is significantly affected by non-radiative recombination process including surface recombination. In order to improve the performance of room temperature mid-infrared LEDs based on narrow bandgap semiconductor, it is necessary to suppress both Auger and SRH recombination. SRH recombination can be greatly reduced by improving the processing of the device whereas one has to modify the device structure suitably using the concept of bandgap engineering in order to reduce Auger recombination at room temperature and under high injection. The model developed here would provide useful design guidelines for the experimentalists for developing new device prototypes.

Acknowledgement

One of the authors (Sanjeev) would like to acknowledge the financial support from the Council for Science and Technology-UP (CST-UP) for this work.

References

[1] A. Krier, Mid-infrared semiconductor optoelectronics, Springer, (2006).
[2] D.A. Pinnow, A.L. Gentile, A.G. Standlee, A.J. Timper, L.M. Hobrock, Appl. Phys. Lett.,**33**, 28 (1978)
[3] L.G. Van Uitert, S.H. Wemple, Appl. Phys. Lett., **33**, 57 (1978)
[4] P.W. France, S.F. Carter, M.W. Moore, C.R. Day, British Telecom Tech J, **5**, 28 (1987)
[5] A. Krier, Phil. Trans. R. Soc. Lond. A, **359**, 599 (2001)
[6] A. Krier, V.V. Sherstnev, J. Phy. D: Appl. Phys., **33**, 101 (2000).
[7] H.H. Gao, A. Krier, V. Sherstnev, Y. Yakovlev, J. Phys. D: Appl. Phys, **32**, 1768 (1999).
[8] A. Krier, X.L. Huang, J. Phys. D: Appl. Phys, **39**, 255 (2006).
[9] A. Krier, M. Stone, S.E. Krier, Semicond. Sci. Technol., **22**, 624 (2007).
[10] B.L. Sharma, R.K. Purohit, Semiconductor Heterojunctions, Pergamon, (1974).
[11] A. Rogalski, K. Adamiec, J. Rutkowski, Narrow- Gap Semiconductor Photodiode, SPIE, (2000).
[12] R. Scholar, S. Price, J. Rosbeck, J. Vacuum Science and Tech. B, **10**, 1507 (1992).
[13] M. Levinshtein, S. Rumyantsev, M. Shur, Handbook Series on Semiconductor Parameters, **1**, World Scientific, (1996).

*Corresponding author: pchakra@bhu.ac.in